The role of a basolateral transporter in rosuvastatin transport and its interplay with apical BCRP in polarized cell monolayer systems

Jibin Li, Ying Wang, Wei Zhang, Yuehua Huang, Kristin Hein and Ismael J. Hidalgo

Absorption Systems, L.P., Exton, Pennsylvania

Running Title:

Rosuvastatin basolateral transport in Caco-2 cells

Corresponding Author: Ismael J. Hidalgo, Ph.D., Absorption Systems LP, 436 Creamery Way, Suite 600, Exton, PA 19341, USA; Phone: (610) 280-7300; Fax: (610) 280-9667; Email: ihidalgo@absorption.com

Text pages:	28
Tables:	4
Figures:	4
References:	39
Words in abstract:	242
Words in introduction:	738
Words in discussion:	1487

Non-standard abbreviations:

A, apical; B, basolateral; BCRP, breast cancer resistance protein; Caco-2, human epithelial colorectal adenocarcinoma cells; DDI, drug-drug interaction; DMEM, Dulbecco's modified Eagle's medium; HBSS, Hanks' balanced salt solution; LC-MS/MS, liquid chromatography with triple quadrupole tandem mass spectrometry; MDCK, Madin-Darby canine kidney cells; MRP2, Multidrug resistance-associated protein 2; OATP, organic anion transporting polypeptide; OST, organic solute transporter; P_{app}, apparent permeability coefficient; P-gp, P-glycoprotein; TEER, transepithelial electrical resistance.

ABSTRACT

Membrane transporters can play a clinically important role in drug absorption and disposition; Caco-2 and MDCK cells are the most widely used *in vitro* models for studying the functions of these transporters and associated drug interactions. Transport studies using these cell models are mostly focused on apical transporters, while basolateral drug transport processes are largely ignored. However, for some hydrophilic drugs, a basolateral uptake transporter may be required for drugs to enter cells before they can interact with apical efflux transporters. The objective of this study was to evaluate potential differences in drug transport across Caco-2 and MDCK basolateral membrane that could cause discrepancy in the identification of efflux transporter substrates and to elucidate the underlying factors that may cause such differences, using rosuvastatin as a model substrate. Bidirectional transport results in Caco-2 and BCRP-MDCK cells demonstrated the necessity of an uptake transporter at the basolateral membrane for rosuvastatin. Kinetic study revealed saturable and nonsaturable processes for rosuvastatin uptake across the Caco-2 basolateral membrane, with the saturable process encompassing >75% of overall rosuvastatin basolateral uptake at concentrations below the K_m (4.2 μM). Furthermore, rosuvastatin basolateral transport exhibited *cis*-inhibition and *trans*-stimulation phenomena, indicating a facilitated diffusion mechanism. This basolateral transporter appeared to be a prerequisite for rosuvastatin and perhaps for other hydrophilic substrates to interact with apical efflux transporters. Deficit of such a basolateral transporter in certain cell models may lead to false negative results when screening drug interactions with apical efflux transporters.

Introduction

Drug transporters play important roles in drug disposition, drug targeting, and particularly transporter-mediated drug-drug interactions (DDIs) (Giacomini and Sugiyama, 2006). Clinical pharmacokinetic DDI studies have suggested that transporters often work together in drug intestinal absorption and hepatic/renal elimination. Uptake and efflux transporters can interact dynamically to mediate drug entry and exit from cells. For example, drug molecules can be taken up across the basolateral membrane of hepatocytes or proximal tubule cells by uptake transporters and subsequently be extruded across the apical membrane into bile or urine by efflux transporters. Given that large number of individuals undergo concurrent, prescription or non-prescription, multi-drug therapy, the potential for transporter-mediated interactions between co-administered drugs is a cause of concern for physicians, the pharmaceutical industry and regulatory agencies (Giacomini et al., 2010). Further, the realization that clinical adverse events involving drug transporters are poorly understood and difficult to predict is fueling an increasing demand for the development of *in vitro* cell systems for DDI prediction.

One of the most extensively utilized *in vitro* cell models for drug transporter assessment has been the human epithelial colorectal adenocarcinoma (Caco-2) cells, which possess many characteristics of intestinal epithelial cells, including intercellular junctional complexes and various uptake and efflux transporters (Artursson and Karlsson, 1991; Hidalgo, 2001; Elsby et al., 2008). Another commonly used *in vitro* cell model is the Madin-Darby canine kidney (MDCK) cells (Polli et al., 2001; Xiao et al., 2006; Kitamura et al., 2008). The latest US FDA draft guidance for drug interaction studies recommends bidirectional permeability assays in either Caco-2 cells or polarized epithelial cell lines overexpressing membrane transporters as a preferred method for *in vitro* determination of whether investigational drugs are substrates of P-gp and/or BCRP (US Department of Health and Human Services et al., 2012). As drug molecules may interact with multiple uptake and efflux transporters naturally expressed *in vivo*,

the missing interplay between apical and basolateral transporters in cell lines expressing a single transporter, by not reflecting the *in vivo* situation, may lead to false negative results. In this regard, Caco-2 cells, a primary-like cell culture that expresses multiple uptake and efflux transporters, appears to be a more appropriate choice of model for this type of study, because it avoids the limitations of singly transfected cells that cannot recapitulate all the mechanisms involved in transcellular transport. As drug transport studies with Caco-2 cells mostly focus on apical transporters, the mechanism of drug translocation across the basolateral membrane is largely ignored. Although a recent publication indicated that OSTα-OSTβ may be involved in the basolateral uptake of taurocholic acid and estrone 3-sulfate in Caco-2 cells (Grandvuinet and Steffansen, 2011) the role of basolateral transporter(s) in Caco-2 cells is not widely appreciated.

The current study explored the basolateral uptake route of drug transport in two different cell systems such as Caco-2 and MDCK cells using rosuvastatin as a model compound. Rosuvastatin is a member of 3-hydroxy-3-methylglutaryl coenzyme A (HMG-CoA) reductase inhibitors (statins), which are among the most widely used drugs worldwide for the treatment and prevention of ischemic heart disease. Rosuvastatin is avidly taken up into hepatocytes, the site of statin action, by multiple active uptake transporters including organic anion transporting polypeptide (OATP) 1B1, 1B3, 2B1, 1A2, and Na^+-taurocholate co-transporting polypeptide (NTCP) transporters at the hepatic sinusoidal membrane (Ho et al., 2006; Choi et al., 2011; Varma et al., 2011). Owing to its hydrophilicity, and ensuing slow passive diffusion across cell membranes, rosuvastatin is liver selective and has a limited distribution into nonhepatic cells. It has been shown that the absolute oral bioavailability of rosuvastatin in humans was ~20% and hepatobiliary excretion appeared to be the predominant elimination route, representing ~70% of total clearance (Martin et al., 2003a). Although two metabolites, rosuvastatin-5S-lactone and N-desmethyl rosuvastatin, have been found, the vast majority of rosuvastatin was excreted unchanged, indicating a minor role of metabolism which presumably involves CYP2C9 (Martin et

al., 2003b).   The clinical significance, organ distribution (primarily governed by multiple transporters), slow biotransformation and passive membrane diffusion of rosuvastatin make it an ideal model compound for drug transporter studies.

In the present study, we examined the bidirectional transport of rosuvastatin across polarized Caco-2 and BCRP-MDCK cell monolayers. The distinct profiles of rosuvastatin transport revealed the existence of basolateral uptake transporter(s) in Caco-2 cells which is deficient in BCRP-MDCK cells. Then we investigated the kinetics and mechanism of rosuvastatin basolateral transport, and interplay between the putative basolateral transporter and apical efflux transporter BCRP in Caco-2 cells.

Materials and Methods

Chemicals. Rosuvastatin calcium was purchased from Toronto Research Chemicals (North York, Ontario, Canada). Dulbecco's modified Eagle's medium (DMEM) was purchased from Life Technologies (Grand Island, NY). Hanks balanced salt solution (HBSS), Fetal bovine serum (FBS) was obtained from Omega (Tarzana, CA). Penicillin-streptomycin, non-essential amino acids (NEAA), sodium pyruvate, and neomycin (G418) were obtained from CellGro (Herndon, VA). Rat tail collagen was purchased from BD Sciences (Bedford, MD). Acetonitrile was purchased from EMD Chemicals (Gibbstown, NJ). Radio-immunoprecipitation assay (RIPA) buffer was obtained from Santa Cruz Biotechnology (Santa Cruz, CA). Bicinchoninic acid (BCA) protein assay kit was purchased from Thermo Pierce (Pittsburgh, PA). Prazosin and all other chemicals were purchased from Sigma Aldrich (St. Louis, MO).

Cell culture. Caco-2 cells and MDCK cells were obtained from American Type Culture Collection (ATCC). The MDCK cells were transfected with pEZ-Lv151 vector (Genecopoeia, Rockville, MD) containing the full length cDNA clone of human ABCG2 wild-type gene (R482) using electroporation method, and stably transfected cells were selected with 800 μg/mL neomycin. For transport study, cells were seeded onto rat tail collagen-coated, microporous, polycarbonate membranes in 12-well Costar Transwell® plates (1.13 cm^2 insert area, 0.4 µm pore size; Corning, NY) at 60,000 cells/cm^2. Cells were maintained in DMEM containing 100 µM NEAA, 1 mM sodium pyruvate, 10% FBS, 100 U/mL penicillin, and 100 µg/mL streptomycin. Neomycin (800 μg/mL) was supplemented to maintain selective pressure for BCRP-MDCK cells. All cells were maintained at 37°C in a humidified atmosphere of 5% CO_2 in air for one week to form confluent monolayers. The culture medium was changed 24 hours after seeding to remove cell debris and dead cells; afterwards the medium was changed every other day. Monolayers were used for transport assays between 21-28 days for Caco-2 cells, and 7-11 days for BCRP-MDCK cells. Cell monolayers were certified based on our internal criteria on

transepithelial electrical resistance (TEER) values, only monolayers met the acceptance criteria (TEER > 450 $\Omega \cdot cm^2$ for Caco-2 and > 1200 $\Omega \cdot cm^2$ for BCRP-MDCK cells) were selected for transport studies.

Transport assays. The transport assay buffer was Hanks' balanced salts solution containing 15 mM glucose (HBSSg), supplemented with 10 mM 2-(N-morpholino)ethanesulfonic acid (MES, pH 5.5) or 10 mM 4-(2-hydroxyethyl)piperazine-1-ethanesulfonic acid (HEPES, pH 7.4). Transport experiments were conducted at apical and basolateral pH 7.4, unless noted otherwise. Bidirectional transport assays in Caco-2 and MDCK cells were carried out by dosing 2 μM rosuvastatin in assay buffer to either the apical compartment (A-to-B) or the basolateral compartment (B-to-A); cells were then incubated at 37°C and samples were collected at 60 and 120 min. Time course study of rosuvastatin B-to-A transport in Caco-2 cells was performed by dosing 10 μM or 200 μM rosuvastatin to the basolateral compartment at 37°C; at pre-selected time points, samples were collected from the apical compartment, cell monolayers were washed twice with ice cold assay buffer and then lysed with acetonitrile on ice for 10 min. Concentration dependency of rosuvastatin basolateral uptake was evaluated by dosing rosuvastatin at various concentrations to the basolateral compartment, cells were incubated at 37°C for 30 min, samples from apical compartment and cell lysates were collected. Inhibition study carried out by measuring 2 μM rosuvastatin B-to-A transport in the absence (control) or presence of the indicated test compounds. *Trans*-stimulation of rosuvastatin basolateral efflux by extracellular taurolithocholate was evaluated by dosing 50 μM rosuvastatin and 10 μM atenolol (low permeability marker) in assay buffer, pH 5.5, to the apical chamber and compound-free (control) or taurolithocholate-containing buffer, pH 7.4, to the basolateral compartment. This high concentration (50 μM) of rosuvastatin was dosed into the apical compartment to overwhelm apical efflux processes as to allow rosuvastatin to reach the intracellular compartment from the apical side. Also, the apical compartment was acidic (pH = 5.5) while the basolateral compartment was close to neutral (pH

8

7.4) to maintain the proton-dependent apical uptake activity of OATP2B1 (Varma et al., 2011).

After dosing, monolayers were incubated at 37°C and samples collected at 15, 30, and 60 min

from the basolateral compartment. In all cases, each determination was performed in triplicate. For

protein analysis, cells were lysed with RIPA buffer and protein concentrations were determined by

BCA protein assay.

Transporter Gene Expression by Real-Time PCR. Real-time quantitative PCR (qPCR)

was performed using the LightCycler® 480 system (Roche Diagnostics, Mannheim, Germany).

Total RNA was isolated from mature cell monolayers using RNeasy® Mini Kit (Qiagen®, Hilden,

Germany) according to the manufacturer's protocol. Synthesis of cDNA was carried out from 1

μg of total RNA using QuantiTect® RT kit (Qiagen®, Hilden, Germany) for reverse transcription-

polymerase chain reaction (PCR) with random hexamer primers according to the manufacturer's

protocol. Primer and probes were designed using the Universal Probe Library (Roche, Basel,

Switzerland). qPCR analysis was performed in 20 μL of reaction mixture containing 10 ng

cDNA, LightCycler® 480 probes master kit with 0.1 μM probe and 0.5 μM primers. The PCR

reaction was run at 95°C for 10 min, followed by 45 amplification cycles of 95°C for 10 s, 60°C

for 15 s, and 72°C for 1 s. Amplification curves were analyzed using LightCycler 480 Basic

Software (version 1.2) which produced threshold cycle time (C_T) values at where fluorescence is

higher than a defined threshold level. Relative gene expression levels of the target genes were

normalized to the expression level of the housekeeping gene β-actin using the formula of $2^{-\Delta C_T}$,

where $\Delta C_T = C_T$ (target gene) $- C_T$ (β-actin).

LC-MS/MS Sample Analyses. Rosuvastatin and prazosin concentrations were determined

using reverse phase liquid chromatography with triple quadruple tandem mass spectrometry (LC-

MS/MS) methods. The HPLC equipment consisted of a Leap CTC HTS PAL autosampler and

Agilent 1100 pumps. Chromatography was performed at ambient temperature using a 30 × 2.1 mm

i.d. 3 μm Thermo Hypersil BDS C18 column with guard column. The mobile phase buffer was 25 mM ammonium formate buffer (pH 3.5); the aqueous reservoir was 90% deionized water and 10% buffer (v/v); the organic reservoir was 90% acetonitrile and 10% buffer. Gradient started at 5% organic and changed linearly over 1.5 to 100% organic phase at a flow rate of 250 μL/min. Injection volume was 20 μL, total run time was 3.5 min. Mass spectrometry was performed on a Sciex® API3000 triple quadruple mass spectrometer in the multiple reaction monitoring modes using a turbo ionspray interface. The Q1/Q3 settings were +482.1/258.3 and +384.5/247.1 for rosuvastatin and prazosin, respectively.

Data Analysis. The apparent permeability coefficient (P_{app}) was calculated using the equation:

$$P_{app} = \frac{dQr/dt}{A \times C_0} \tag{1}$$

where dQr/dt is the cumulative drug amount transported into the receiver compartment (Qr) over time (t) during transport experiment, A is the area of cell monolayer, and C_0 is the initial concentration in the donor compartment. The efflux ratio (ER) was calculated as the ratio of the P_{app} measured in the B-to-A direction divided by the P_{app} in the A-to-B direction.

Kinetic analysis of rosuvastatin basolateral uptake in Caco-2 at 37°C was performed by nonlinear regression analysis using GraphPad Prism 5.0 (GraphPad Software Inc., San Diega, CA). The data were fit to a model containing a saturable and nonsaturable term (Ming et al., 2011):

$$J = \frac{J_{max} \cdot C}{K_m + C} + K_d \cdot C \tag{2}$$

where J is the uptake rate normalized to protein, J_{max} is the maximal uptake rate, K_m is the Michaelis constant for the saturable uptake, K_d is a constant for the nonsaturable uptake, and C is the initial concentration in the donor compartment.

Statistical Analysis. Statistical analysis was performed using GraphPad Prism (version 5.04 for Windows, GraphPad Software Inc., San Diego, CA). Statistical significance was evaluated using Student's *t* test (unpaired, two tailed) for two-group comparison or one-way analysis of variance (ANOVA) followed by post hoc Tukey tests for more than two group comparison. Differences with $p < 0.05$ were considered statistically significant.

Results

Different transport profiles of rosuvastatin in Caco-2 and BCRP-MDCK cells.
Rosuvastatin exhibited high efflux in Caco-2 cells, as evidenced by an ER of 83, and moderate efflux in BCRP-MDCK cells, which had an ER of 5.8 (Table 1). Although rosuvastatin transport in the A-to-B direction was low in both Caco-2 and BCRP-MDCK cells (0.25 and 0.28 $\times 10^{-6}$ cm/s), B-to-A transport in Caco-2 cells was 12-fold higher than B-to-A transport in BCRP-MDCK (20.66 vs 1.63 $\times 10^{-6}$ cm/s). To confirm the BCRP functionality in BCRP-MDCK cells, we determined the bidirectional permeability of prazosin, a prototypical BCRP probe substrate (Xiao et al., 2006; Giri et al., 2009; Mittapalli et al., 2012). Prazosin was highly efflux in both cell lines (Table 1), but differences in transport patterns were observed. B-to-A transport rates were comparable (45 $\times 10^{-6}$ cm/s in BCRP-MDCK vs. 41 $\times 10^{-6}$ cm/s in Caco-2); however, due to a lower A-to-B transport in BCRP-MDCK cells, the ER was 3 times higher in BCRP-MDCK (34.5 in BCRP-MDCK vs. 10.5 in Caco-2).

Transporter-mediated basolateral uptake of rosuvastatin in Caco-2 cells. To determine whether the discrepancy in rosuvastatin transport between Caco-2 and BCRP-MDCK could be explained by the presence in Caco-2 cells, and absence in BCRP-MDCK cells, of a basolateral uptake transporter, we undertook the characterization of this putative transporter in Caco-2 monolayers. The rate of B-to-A transport and extent of cellular accumulation of rosuvastatin were roughly linear between 10 and 200 μM (Fig. 1). At pre-selected time points, the amount of rosuvastatin associated with the cells and the amount released into the apical compartment were added up to determine the total amount of rosuvastatin taken up across the basolateral membrane. Considering that the transport rate was linear at 30 minutes, and that the lower receiver chamber concentrations at earlier time points would increase analytical variability, we decided to measure total rosuvastatin basolateral uptake rates at 30 min. The rosuvastatin basolateral uptake rates were concentration dependent (Fig. 2) and best fit to a

modified Michaelis-Menten model with saturable and nonsaturable process. The apparent Michaelis-Menten constant, K_m, the saturable maximal flux, J_{max}, and the passive diffusion coefficient, K_d were estimated to be 4.212 ± 2.130 µM, 24.64 ± 6.10 pmol min^{-1} mg protein^{-1}, and 0.9985 ± 0.1162 µL min^{-1} mg protein^{-1}, respectively.

Expression of organic anion transporter mRNA in Caco-2 cells. Rosuvastatin has an estimated pK_a of 4.2-4.6 (Varma et al., 2011) and exists primarily as an organic anion at physiological pH. OATP1A2, OATP1B1, OATP1B3, and OATP2B1 have been shown to mediate the uptake of rosuvastatin (Ho et al., 2006; Varma et al., 2011). The heteromeric organic solute transporter (OSTα-OSTβ), identified as a major basolateral bile acid and steroid transporter in human intestinal epithelia (Ballatori et al., 2005), is the only basolateral exchanger known to transport organic anions (Grandvuinet and Steffansen, 2011). Thus, through the use of real-time PCR, we determined the mRNA expression levels in Caco-2 cells of the transporters commonly associated with the transport of organic anionic molecules. As shown in Table 2, Caco-2 cells express the genes of OATP1A2, OATP2B1, OSTα, and OSTβ but not OATP1B1 and OATP1B3.

Cis-inhibition and _trans_-stimulation of rosuvastatin basolateral transport in Caco-2 cells. To further investigate the possibility of OSTα-OSTβ involvement in rosuvastatin basolateral transport, inhibition of rosuvastatin B-to-A transport was evaluated in the presence of a series of compounds known to interact with OSTα-OSTβ (Seward et al., 2003; Ballatori et al., 2005). When co-dosed with rosuvastatin into the basolateral compartment, all the tested bile salts, steroid conjugates, and organic anions caused significantly _cis_-inhibition of the basolateral uptake of rosuvastatin (Table 3). The basolateral efflux of rosuvastatin from cells was measured in the absence (control) and presence of taurolithocholate in the basolateral compartment. In the absence of taurolithocholate, rosuvastatin basolateral efflux was 14.24 ± 0.34 pmol min^{-1} mg protein^{-1}; when taurolithocholate was present in the basolateral compartment, rosuvastatin basolateral efflux increased by more than 3 folds (Table 4). The transport of a low permeability

marker, atenolol, co-dosed along with rosuvastatin to ensure the integrity of Caco-2 monolayers, showed no significant differences under these assay conditions, indicating that the barrier properties of the Caco-2 monolayers were not compromised.

Cooperative action of basolateral uptake and apical efflux transporters in rosuvastatin B-to-A transport. Our concept of the B-to-A transport process of rosuvastatin across Caco-2 cell monolayers is portrayed in a simplified schematic model (Fig. 3), in which rosuvastatin is taken up into the cell by a basolateral uptake transporter and then excreted across the apical membrane by an apical efflux transporter. Based on this model, inhibition of the basolateral transporter would reduce the B-to-A transport and intracellular accumulation of rosuvastatin, whereas inhibition of the apical efflux transporter would also decrease rosuvastatin B-to-A transport but would increase its intracellular accumulation. To test the hypothesis, we used estrone 3-sulfate and rifamycin SV to inhibit the basolateral transporter (OSTα-OSTβ), and Ko143 and novobiocin to inhibit BCRP-mediated apical efflux in Caco-2 cells. While all four compounds significantly reduced rosuvastatin B-to-A transport (Fig. 4A), estrone 3-sulfate and rifamycin SV decreased the intracellular accumulation of rosuvastatin, whereas Ko143 and novobiocin increased it (Fig. 4B).

Discussion

Rosuvastatin is well known to be transported by BCRP *in vitro* (Huang et al., 2006; Deng et al., 2008; Li et al., 2011) and *in vivo* (Zhang et al., 2006; Keskitalo et al., 2009). In the current study, rosuvastatin was effectively effluxed in Caco-2 cells, with an efflux ratio (ER) of 83, but only mildly effluxed in BCRP-MDCK, with an ER of 5.8 (Table 1). Although one possible reason for the reduced rosuvastatin transport in BCRP-MDCK cells could be low BCRP functionality in BCRP-MDCK cells, the transport data of BCRP substrate prazosin rules out this possibility. Rosuvastatin, with an estimated pK_a of 4.2-4.6 (Varma et al., 2011), exists primarily in the anionic form at physiological pH, and its pH-partition driven permeability component can be considered negligible. Indeed, rosuvastatin transport in wild type MDCK cells was extremely low in both directions. As MDCK cells express little transport activity, these values reflect the low intrinsic membrane permeability of rosuvastatin. These observations suggest that low apical efflux of rosuvastatin in BCRP-MDCK is not due to lack of BCRP function but rather reflects deficient basolateral uptake, and rosuvastatin efflux in Caco-2 is likely enhanced by a concerted action of basolateral uptake transporter(s) and apical efflux transporters. One implication of this difference is that the use of BCRP-MDCK cells alone to study drug interactions with BCRP could lead to erroneous results for hydrophilic molecules, which require a basolateral uptake transporter (Kitamura et al., 2008). Thus, this study was set forth to investigate the transport mechanism(s) in Caco-2 cells responsible for rosuvastatin basolateral uptake. Although rosuvastatin was used as a model compound, this type of studies would have application to other drugs and other transporters that may be involved in carrier-mediated transepithelial drug transport.

First we examined rosuvastatin transport across Caco-2 cell monolayers in the B-to-A direction (Fig. 1). The B-to-A transport of rosuvastatin dosed at 10 and 200 μM was initially linear up to 30 min, after which it further increased. The nonlinear increase in rosuvastatin B-to-

15

A transport after 30 min may be due to progressive engagement of the apical efflux transporters (P-gp, BCRP, or MRP2) when increasing amount of intracellular rosuvastatin reached the apical membrane. The amount of rosuvastatin released into the apical compartment, in a 2-hr experiment, was much higher than the amount retained inside the cell. Such results indicate that the apical efflux transporters efficiently vacuumed the drug from the intracellular compartment, and it can be concluded that basolateral uptake is the rate-limiting step in the B-to-A rosuvastatin transport. Concentration-dependence experiments showed that rosuvastatin basolateral uptake consisted of saturable and nonsaturable processes (Fig. 2) and kinetic analysis revealed that at concentrations below K_m the saturable process accounts for more than 75% of the total uptake. These data provided direct experimental evidence that a transporter was involved in rosuvastatin basolateral uptake.

While these data indicated that a basolateral uptake transporter was involved, the identity of this transporter was unclear. Multiple active uptake transporters expressed at the hepatic sinusoidal membrane have been shown to mediate the hepatic uptake of rosuvastatin, including OATP1B1, OATP1B3, OATP2B1, OATP1A2, and NTCP (Ho et al., 2006; Choi et al., 2011; Varma et al., 2011). OATP1B1 and OATP1B3, believed to be liver-specific, are primarily expressed on the sinusoidal membrane of human hepatocytes (Abe et al., 1999; König et al., 2000). In addition, our qPCR results (Table 2) and a previous study (Hayeshi et al., 2008) showed that Caco-2 cells do not express OATP1B1 or OATP1B3 mRNAs. Although NTCP mRNAs were detected in Caco-2 cells from certain laboratories, the expression levels were low and even absent in some cell sources (Hilgendorf et al., 2007; Hayeshi et al., 2008). Furthermore, in contrast to MDCK cells, Caco-2 failed to sort recombinant NTCP-GFP protein into polarized surface expression on the plasma membrane and showed no polarity of taurocholate uptake (Sun et al., 2001), thus suggesting a lack of meaningful NTCP protein expression and function in Caco-2 systems. Both OATP1A2 and OATP2B1 are expressed at

16

the apical membrane of enterocytes or Caco-2 cells (Sai et al., 2006; Glaeser et al., 2007), where they can contribute to the absorption of drugs such as statins, fexofenadine, levofloxacin, methotrexate, and talinolol (Badagnani et al., 2006; Ho et al., 2006; Maeda et al., 2007; Kitamura et al., 2008; Shirasaka et al., 2010; Ming et al., 2011). For the aforementioned reasons, it is highly unlikely that OATP1B1, OATP1B3, OATP2B1, OATP1A2, or NTCP could be involved in the basolateral uptake of rosuvastatin in Caco-2 cells. As a result, basolateral OSTα-OSTβ transporter was singled out as the most likely candidate among known transporters for facilitating rosuvastatin penetration across the basolateral membrane. OSTα-OSTβ heteromeric exchanger transports substrates in both directions across the cell membrane (i.e. uptake and efflux) via a facilitated diffusion mechanism (Ballatori et al., 2005). Challenging rosuvastatin basolateral uptake with OSTα-OSTβ inhibitors (Seward et al., 2003) caused significant *cis*-inhibition, which indicates the likelihood of OSTα-OSTβ involvement. Next, we investigated the directionality of rosuvastatin basolateral transport to further characterize the mechanism of this basolateral transport system. Since OSTα-OSTβ is a membrane exchanger (Ballatori et al., 2005), if rosuvastatin basolateral transport is indeed mediated by OSTα-OSTβ this process is expected to be bi-directional and susceptible to *trans*-stimulation. A large increase in basolateral efflux when taurolithocholate was present in the opposite side of cell membrane (i.e. *trans*-stimulation) supports the involvement of OSTα-OSTβ in rosuvastatin basolateral transport in Caco-2 cells.

The finding that rosuvastatin is transported across basolateral membrane by a facilitated diffusion in Caco-2 cells could shed light on rosuvastatin intestinal absorption *in vivo*. Given the hydrophilic nature and limited membrane permeability of rosuvastatin, it is likely that rosuvastatin intestinal absorption, estimated to be about 50% (Martin et al., 2003a), involves apical uptake and basolateral efflux (or exchange) transporters. A recent report showed that rosuvastatin underwent OATP2B1-mediated apical uptake in Caco-2 cells (Varma et al., 2011), it is conceivable that the

intestinal absorption of rosuvastatin *in vivo* involves apical uptake transporter(s) and basolateral exchange/efflux transporter(s). After a usual dose of 20 mg, the maximum plasma concentration (C_{max}) of rosuvastatin ranged from 0.006 to 0.03 µM in healthy male volunteers (Zhang et al., 2006), which are well below the K_m value of 4.2 µM determined for the basolateral transporter in Caco-2 cells; thus, this transporter can undertake the facilitated basolateral transport of rosuvastatin *in vivo*. However, the intestinal disposition of rosuvastatin has not been fully delineated yet; additional studies are needed to clarify the roles of OATP2B1 and OSTα-OSTβ in rosuvastatin transport across the intestinal epithelium. One approach that could furnish unambiguous identification of transporter involvement is the use of RNA interference to knock down the expression of relevant transporters. This technique has already been used to selectively knock down the expression of BCRP, P-gp and MRP2 in Caco-2 cells (Zhang et al., 2009), which proved valuable in elucidating the role of efflux transporters in the biliary efflux of ximelagatran (Darnell et al., 2010) and several statin drugs (Li et al., 2011).

Lastly, we investigated the cooperative action of this basolateral uptake transporter with apical BCRP involved in rosuvastatin B-to-A transport. Based on our conceptual model (Fig. 3), it is possible to tease out the role of the basolateral transporter from the apical efflux transporter. The model predicts that inhibition of the apical efflux transporter would increase the intracellular accumulation of rosuvastatin, whereas inhibition of the basolateral uptake transporter would reduce the intracellular accumulation. Thus to test the prediction of a cooperative interaction between the basolateral uptake transporter and apical BCRP, we determined rosuvastatin B-to-A transport in the presence of estrone 3-sulfate or rifamycin SV (inhibitors of basolateral OSTα-OSTβ), and in the presence of Ko143 or novobiocin (inhibitors of apical BCRP). Results show that all four compounds inhibited rosuvastatin overall B-to-A transport, but estrone 3-sulfate and rifamycin SV reduced intracellular accumulation while Ko143 and novobiocin increased it, demonstrating a functional interaction between the basolateral transporter and apical BCRP for

rosuvastatin B-to-A transport in Caco-2 cells. It was noticed that although novobiocin produced greater inhibition on rosuvastatin B-to-A flux than Ko143, it caused less intracellular accumulation. One possible explanation is that novobiocin also partially inhibits the basolateral uptake transporter, as cross-inhibition is a common difficulty associated with transporter studies using chemical inhibitors (Watanabe et al., 2005; Wang et al., 2008).

In conclusion, this study sought to investigate the distinct rosuvastatin transport profiles: robust apical efflux in Caco-2 cells but much reduced efflux in BCRP-MDCK cells. Through a series of transport experiments the role of a basolateral transporter facilitating the basolateral penetration of rosuvastatin to access apical efflux transporters was revealed in Caco-2 cells, and our data suggest that the OSTα-OSTβ heteromeric exchanger is likely involved. Further investigations are needed to achieve a definitive characterization of this basolateral transporter with respect to molecular identity and substrate selectivity. Such research is of value because the use of cell monolayer systems lacking such a transporter may lead to false negative recognition of potentially important drug-transporter interactions.

Acknowledgments

Authorship contributions

Participated in research design: Li, Wang, Zhang and Hidalgo

Conducted experiments: Wang and Hein

Contributed new reagents or analytic tools: Huang

Performed data analysis: Wang and Li

Wrote or contributed to the writing of the manuscript: Li, Wang, and Hidalgo

References

Abe T, Kakyo M, Tokui T, Nakagomi R, Nishio T, Nakai D, Nomura H, Unno M, Suzuki M, Naitoh T, Matsuno S, and Yawo H (1999) Identification of a novel gene family encoding human liver-specific organic anion transporter LST-1. *J Biol Chem* **274:**17159-17163.

Artursson P and Karlsson J (1991) Correlation between oral drug absorption in humans and apparent drug permeability coefficients in human intestinal epithelial (Caco-2) cells. *Biochem Biophys Res Commun* **175:**880-885.

Badagnani I, Castro RA, Taylor TR, Brett CM, Huang CC, Stryke D, Kawamoto M, Johns SJ, Ferrin TE, Carlson EJ, Burchard EG, and Giacomini KM (2006) Interaction of methotrexate with organic-anion transporting polypeptide 1A2 and its genetic variants. *J Pharmacol Exp Ther* **318:**521-529.

Ballatori N, Christian WV, Lee JY, Dawson PA, Soroka CJ, Boyer JL, Madejczyk MS, and Li N (2005) OSTα-OSTβ: a major basolateral bile acid and steroid transporter in human intestinal, renal, and biliary epithelia. *Hepatology* **42:**1270-1279.

Choi MK, Shin HJ, Choi YL, Deng JW, Shin JG, and Song IS (2011) Differential effect of genetic variants of Na$^+$-taurocholate co-transporting polypeptide (NTCP) and organic anion-transporting polypeptide 1B1 (OATP1B1) on the uptake of HMG-CoA reductase inhibitors. *Xenobiotica* **41:**24-34.

Darnell M, Karlsson JE, Owen A, Hidalgo IJ, Li J, Zhang W, and Andersson TB (2010) Investigation of the involvement of P-glycoprotein and multidrug resistance-associated protein 2 in the efflux of ximelagatran and its metabolites by using short hairpin RNA knockdown in Caco-2 cells. *Drug Metab Dispos* **38:**491-497.

Deng JW, Shon JH, Shin HJ, Park SJ, Yeo CW, Zhou HH, Song IS, and Shin JG (2008) Effect of silymarin supplement on the pharmacokinetics of rosuvastatin. *Pharm Res* **25:**1807-1814.

Elsby R, Surry DD, Smith VN, and Gray AJ (2008) Validation and application of Caco-2 assays for the in vitro evaluation of development candidate drugs as substrates or inhibitors of P-glycoprotein to support regulatory submissions. *Xenobiotica* **38:**1140-1164.

Giacomini KM, Huang SM, Tweedie DJ, Benet LZ, Brouwer KL, Chu X, Dahlin A, Evers R, Fischer V, Hillgren KM, Hoffmaster KA, Ishikawa T, Keppler D, Kim RB, Lee CA, Niemi M, Polli JW, Sugiyama Y, Swaan PW, Ware JA, Wright SH, Wah Yee S, Zamek-Gliszczynski MJ, and Zhang L (2010) Membrane transporters in drug development. *Nat Rev Drug Discov* **9:**215-236.

Giacomini KM and Sugiyama Y (2006) Membrane transporters and drug response, in: *Goodman & Gilman's the pharmacological basis of therapeutics* (Goodman LS, Gilman A, Brunton LL, Lazo JS and Parker K eds), pp 41-70, McGraw-Hill, New York.

Giri N, Agarwal S, Shaik N, Pan G, Chen Y, and Elmquist WF (2009) Substrate-dependent breast cancer resistance protein (Bcrp1/Abcg2)-mediated interactions: consideration of multiple binding sites in in vitro assay design. *Drug Metab Dispos* **37:**560-570.

Glaeser H, Bailey DG, Dresser GK, Gregor JC, Schwarz UI, McGrath JS, Jolicoeur E, Lee W, Leake BF, Tirona RG, and Kim RB (2007) Intestinal drug transporter expression and the impact of grapefruit juice in humans. *Clin Pharmacol Ther* **81:**362-370.

Grandvuinet AS and Steffansen B (2011) Interactions between organic anions on multiple transporters in Caco-2 cells. *J Pharm Sci* **100:**3817-3830.

Hayeshi R, Hilgendorf C, Artursson P, Augustijns P, Brodin B, Dehertogh P, Fisher K, Fossati L, Hovenkamp E, Korjamo T, Masungi C, Maubon N, Mols R, Müllertz A, Mönkkönen J, O'Driscoll C, Oppers-Tiemissen HM, Ragnarsson EG, Rooseboom M, and Ungell AL (2008) Comparison of drug transporter gene expression and functionality in Caco-2 cells from 10 different laboratories. *Eur J Pharm Sci* **35:**383-396.

Hidalgo IJ (2001) Assessing the absorption of new pharmaceuticals. *Curr Top Med Chem* **1:**385-401.

Hilgendorf C, Ahlin G, Seithel A, Artursson P, Ungell AL, and Karlsson J (2007) Expression of thirty-six drug transporter genes in human intestine, liver, kidney, and organotypic cell lines. *Drug Metab Dispos* **35:**1333-1340.

Ho RH, Tirona RG, Leake BF, Glaeser H, Lee W, Lemke CJ, Wang Y, and Kim RB (2006) Drug and bile acid transporters in rosuvastatin hepatic uptake: function, expression, and pharmacogenetics. *Gastroenterology* **130:**1793-1806.

Huang L, Wang Y, and Grimm S (2006) ATP-dependent transport of rosuvastatin in membrane vesicles expressing breast cancer resistance protein. *Drug Metab Dispos* **34:**738-742.

Keskitalo JE, Zolk O, Fromm MF, Kurkinen KJ, Neuvonen PJ, and Niemi M (2009) ABCG2 polymorphism markedly affects the pharmacokinetics of atorvastatin and rosuvastatin. *Clin Pharmacol Ther* **86:**197-203.

Kitamura S, Maeda K, Wang Y, and Sugiyama Y (2008) Involvement of multiple transporters in the hepatobiliary transport of rosuvastatin. *Drug Metab Dispos* **36:**2014-2023.

König J, Cui Y, Nies AT, and Keppler D (2000) Localization and genomic organization of a new hepatocellular organic anion transporting polypeptide. *J Biol Chem* **275:**23161-23168.

Li J, Volpe DA, Wang Y, Zhang W, Bode C, Owen A, and Hidalgo IJ (2011) Use of transporter knockdown Caco-2 cells to investigate the in vitro efflux of statin drugs. *Drug Metab Dispos* **39:**1196-1202.

Maeda T, Takahashi K, Ohtsu N, Oguma T, Ohnishi T, Atsumi R, and Tamai I (2007) Identification of influx transporter for the quinolone antibacterial agent levofloxacin. *Mol Pharm* **4:**85-94.

Martin PD, Warwick MJ, Dane AL, Brindley C, and Short T (2003a) Absolute oral bioavailability of rosuvastatin in healthy white adult male volunteers. *Clin Ther* **25:**2553-2563.

Martin PD, Warwick MJ, Dane AL, Hill SJ, Giles PB, Phillips PJ, and Lenz E (2003b) Metabolism, excretion, and pharmacokinetics of rosuvastatin in healthy adult male volunteers. *Clin Ther* **25:**2822-2835.

Ming X, Knight BM, and Thakker DR (2011) Vectorial Transport of Fexofenadine across Caco-2 Cells: Involvement of Apical Uptake and Basolateral Efflux Transporters. *Mol Pharm* **8:**1677-1686.

Mittapalli RK, Vaidhyanathan S, Sane R, and Elmquist WF (2012) Impact of P-glycoprotein (ABCB1) and Breast Cancer Resistance Protein (ABCG2) on the Brain Distribution of a novel B-RAF Inhibitor: Vemurafenib (PLX4032). *J Pharmacol Exp Ther*.

Polli JW, Wring SA, Humphreys JE, Huang L, Morgan JB, Webster LO, and Serabjit-Singh CS (2001) Rational use of in vitro P-glycoprotein assays in drug discovery. *J Pharmacol Exp Ther* **299:**620-628.

Sai Y, Kaneko Y, Ito S, Mitsuoka K, Kato Y, Tamai I, Artursson P, and Tsuji A (2006) Predominant contribution of organic anion transporting polypeptide OATP-B (OATP2B1) to apical uptake of estrone-3-sulfate by human intestinal Caco-2 cells. *Drug Metab Dispos* **34:**1423-1431.

Seward DJ, Koh AS, Boyer JL, and Ballatori N (2003) Functional complementation between a novel mammalian polygenic transport complex and an evolutionarily ancient organic solute transporter, OSTα-OSTβ. *J Biol Chem* **278:**27473-27482.

Shirasaka Y, Kuraoka E, Spahn-Langguth H, Nakanishi T, Langguth P, and Tamai I (2010) Species difference in the effect of grapefruit juice on intestinal absorption of talinolol between human and rat. *J Pharmacol Exp Ther* **332:**181-189.

Sun AQ, Swaby I, Xu S, and Suchy FJ (2001) Cell-specific basolateral membrane sorting of the human liver Na$^+$-dependent bile acid cotransporter. *Am J Physiol Gastrointest Liver Physiol* **280:**G1305-1313.

US Department of Health and Human Services, Food and Drug Administration, and Center of Drug Evaluation and Research (CDER) (2012) Draft Guidance for Industry. Drug Interaction Studies - Study design, Data Analysis, Implications for Dosing, and Labeling Recommendations. *US FDA website* *[online],* http://www.fda.gov/downloads/Drugs/GuidanceComplianceRegulatoryInformation/Guidances/UCM292362.pdf.

Varma MV, Rotter CJ, Chupka J, Whalen KM, Duignan DB, Feng B, Litchfield J, Goosen TC, and El-Kattan AF (2011) pH-sensitive interaction of HMG-CoA reductase inhibitors (statins) with organic anion transporting polypeptide 2B1. *Mol Pharm* **8:**1303-1313.

Wang Q, Strab R, Kardos P, Ferguson C, Li J, Owen A, and Hidalgo IJ (2008) Application and limitation of inhibitors in drug-transporter interactions studies. *Int J Pharm* **356:**12-18.

Watanabe T, Onuki R, Yamashita S, Taira K, and Sugiyama Y (2005) Construction of a functional transporter analysis system using MDR1 knockdown Caco-2 cells. *Pharm Res* **22:**1287-1293.

Xiao Y, Davidson R, Smith A, Pereira D, Zhao S, Soglia J, Gebhard D, de Morais S, and Duignan DB (2006) A 96-well efflux assay to identify ABCG2 substrates using a stably transfected MDCK II cell line. *Mol Pharm* **3:**45-54.

Zhang W, Li J, Allen SM, Weiskircher EA, Huang Y, George RA, Fong RG, Owen A, and Hidalgo IJ (2009) Silencing the breast cancer resistance protein expression and function in caco-2 cells using lentiviral vector-based short hairpin RNA. *Drug Metab Dispos* **37:**737-744.

Zhang W, Yu BN, He YJ, Fan L, Li Q, Liu ZQ, Wang A, Liu YL, Tan ZR, Fen J, Huang YF, and Zhou HH (2006) Role of BCRP 421C>A polymorphism on rosuvastatin pharmacokinetics in healthy Chinese males. *Clin Chim Acta* **373:**99-103.

Legends for figures

FIG. 1.   Time course of rosuvastatin B-to-A transport in Caco-2 cells. The symbol of open triangle represents the drug amount retained inside the cell, the open circular represents the drug released into the apical compartment, and the close circle is the sum of the drug retained inside the cell and released into the apical compartment. Each point represents the mean ± S.D., $n = 3$.

FIG. 2.   Concentration-dependent uptake of rosuvastatin across Caco-2 basolateral membrane. Results are represented with the fitted uptake data (——), the saturable (– – –) and nonsaturable (······) transport components. Values are expressed as the mean ± S.D., $n = 3$.

FIG. 3.   Model for the proposed rosuvastatin B-to-A transport across Caco-2 cell monolayers. Left, rosuvastatin is taken up by a basolateral transporter from the basal membrane and excreted by apical efflux transporters at the apical membrane; middle, blocking the basolateral transporter reduces rosuvastatin B-to-A transport and cellular accumulation; right, blocking the apical efflux transporter reduces rosuvatatin B-to-A transport but increases its intracellular accumulation.

FIG. 4.   Effects of selected chemicals on rosuvastatin B-to-A transport in Caco-2 cells. B-to-A transport of 2 µM rosuvastatin was conducted in the absence (control) or the presence of selected inhibitors: 50 µM estrone 3-sulfate (E3S), 50 µM rifamycin SV (Rif SV), 2 µM Ko143, or 10 µM novobiocin (Novo). A, B-to-A transepithelial flux; B, B-to-A intracellular accumulation. Each bar represents the mean ± S.D.; $n = 3$.

TABLE 1

Permeabilities of rosuvastatin and prazosin in Caco-2, MDCK, and BCRP-MDCK cells

Data are expressed as mean ± S.D. ($n = 3$).

Cell Line	Rosuvastatin			Prazosin		
	A-to-B P_{app}	B-to-A P_{app}	ER	A-to-B P_{app}	B-to-A P_{app}	ER
	$\times 10^{-6}$ cm/s			$\times 10^{-6}$ cm/s		
Caco-2	0.25 ± 0.08	20.66 ± 3.47	83.2	3.92 ± 0.28	41.10 ± 5.30	10.5
MDCK	0.43 ± 0.11	0.49 ± 0.14***	1.1	4.32 ± 0.31	13.57 ± 2.07**	3.1
BCRP-MDCK	0.28 ± 0.09	1.63 ± 0.09***	5.8	1.31 ± 0.35	45.15 ± 0.45 (NS)	34.5

**, $p < 0.01$ and ***, $p < 0.001$ significance level of the difference from the B-to-A transport in Caco-2.

N.S., not statistically different from the B-to-A transport in Caco-2.

TABLE 2

Relative mRNA expression of organic anion transporters in Caco-2 cells

Data are expressed as mean ± S.D. (*n* = 3).

Common name	Gene symbol	Accession I.D.	Primer sequence		Amplicon length (bp)	Relative mRNA expression (per million β-actin)		
			Forward	Reverse				
OATP1A2	SLCO1A2	NM_134431	5'- ggggcatgcaggatatatga-3'	5'-tggaacaaagcttgatcctctta-3'	77	101	±	6
OATP1B1	SLCO1B1	NM_006446	5'-ttcaagtggcaataaaaagccta-3'	5'-cacccaaatgggctgagtaa-3'	95	undetectable		
OATP1B3	SLCO1B3	NM_019844	5'-ccatcactcaaatagaaaggagatt-3'	5'-acaatcacaagcaaatttccaa-3'	94	undetectable		
OATP2B1	SLCO2B1	NM_007256	5'-ggcgaaaggtcttagcagtc-3'	5'-gcttagagggagagtccttgc-3'	63	2702	±	157
OSTα	OSTalpha	NM_152672	5'-ctgaagaccaattacggcatc-3'	5'-gagggcaagttccacagg-3'	96	529	±	89
OSTβ	OSTbeta	NM_178859	5'-gctgtggtggtcattataagcat-3'	5'-gtggctgcatcgtttctttt-3'	76	5885	±	299
β-Actin	ACTB	NM_001101	5'-attggcaatgagcggttc-3'	5'-ggatgccacaggactccat-3'	95	Control		

26

TABLE 3

Cis-inhibition of rosuvastatin basolateral uptake in Caco-2 cells.

Rosuvastatin (2 μM) was co-dosed with the indicated compounds into the basolateral compartment at pH 7.4, intracellular uptake was measured. Data are expressed as mean ± S.D. (n = 3).

Treatment	Basolateral uptake[a] (pmol min^{-1} mg protein^{-1})		% Control
Bile salts			
Control	13.74 ±	1.13	100
+ Chenodeoxycholate, 200 μM	3.83 ±	0.30***	27.9
+ Lithocholate acid, 200 μM	5.86 ±	0.32***	42.6
+ Taurocholate, 200 μM	4.00 ±	0.44***	29.1
+ Taurolithocholate, 200 μM	4.14 ±	0.22***	30.1
Steroids			
+ Dehydroepiandrosterone sulfate, 200 μM	5.24 ±	0.10***	38.1
+ Digoxin, 200 μM	6.04 ±	0.16***	43.9
+ Estrone 3-sulfate, 200 μM	3.95 ±	0.56***	28.7
+ Spironolactone, 200 μM	4.82 ±	0.45***	35.1
Organic anions			
+ Bromosulfophthalein, 200 μM	3.23 ±	0.23***	23.5
+ Indomethacin, 200 μM	4.49 ±	0.42***	32.7
+ Probenecid, 1 mM	10.14 ±	1.85***	73.8
+ Rifamycin SV, 50 μM	2.94 ±	0.52***	21.4

***, $p < 0.001$, significance level of the difference from the control.

TABLE 4

Trans-stimulation of rosuvastatin basolateral efflux in Caco-2 cells.

Rosuvastatin (50 μM) and atenolol (10 μM) were co-dosed into the apical compartment at pH 5.5; rosuvastatin release in the basolateral compartment at pH 7.4 was measured in the absence (control) or the presence taurolithocholate. Data are expressed as mean ± S.D. ($n = 3$).

Treatment	Basolateral efflux[a] (pmol min^{-1} mg protein^{-1})	% Control
Control	14.24 ± 0.34	100
+ Taurolithocholate, 10 μM	48.16 ± 13.68***	338
+ Taurolithocholate, 50 μM	62.12 ± 12.34***	436
+ Taurolithocholate, 100 μM	51.17 ± 7.13***	359

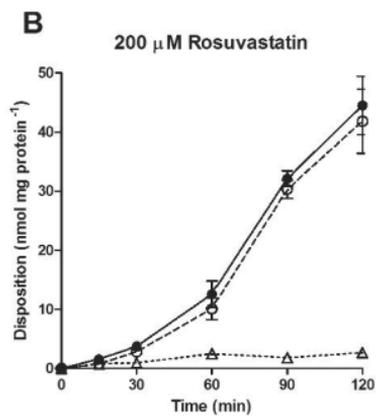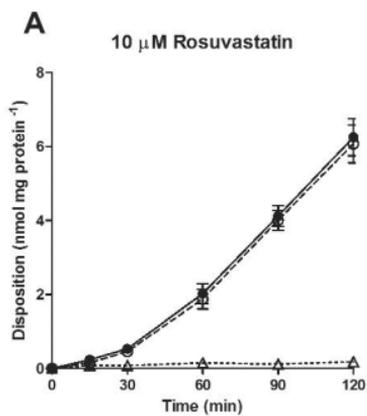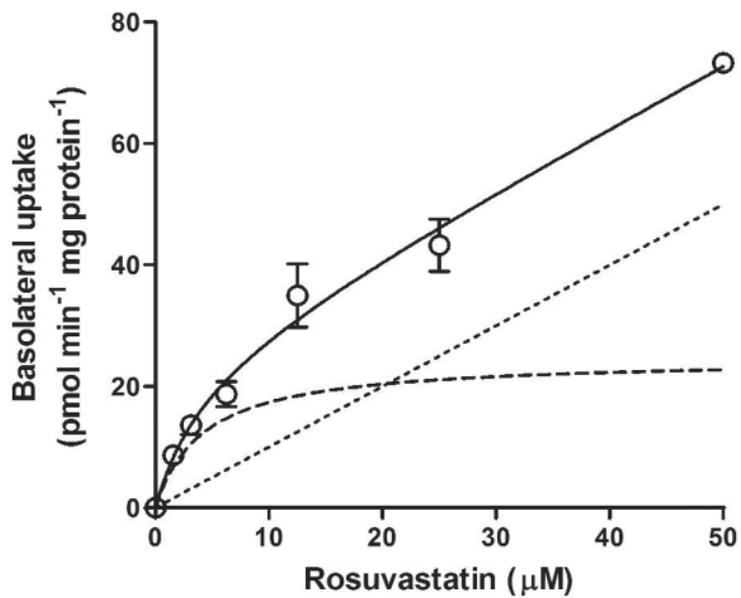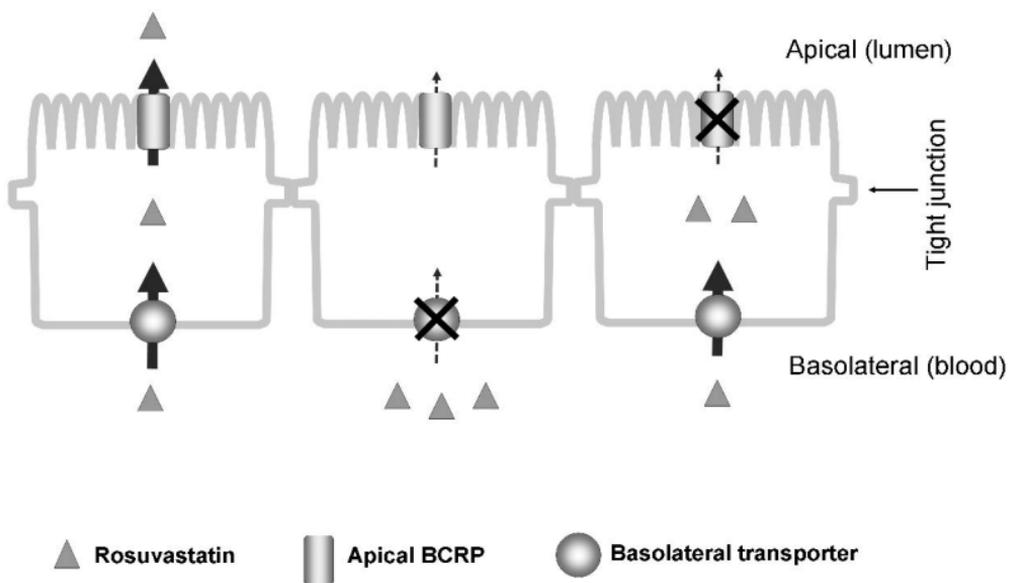***, $p < 0.001$, significance level of the difference from the control.

FIG 1

A 10 μM Rosuvastatin

B 200 μM Rosuvastatin

FIG 2

FIG 3

Apical (lumen)

Tight junction

Basolateral (blood)

△ Rosuvastatin   ▯ Apical BCRP   ● Basolateral transporter

FIG 4